

Diffusion, Excitons and Adsorptivity of H and He atoms on KBr (001) M-center Surface: DFT calculations.

Kh. M. Eid

Department of Physics, Faculty of Education, Ain Shams University, Cairo, Egypt

The energetic properties of M-center diffusion, excitons near M^{2+} , M^+ , M , M^- and M^{2-} centers and adsorptivity of H and He atoms over defect free and defect containing surfaces of KBr using Density Functional Theory (DFT) calculations are discussed. The results clarify that: (i) The calculated barriers for diffusing M-center in its lowest triplet excited state is similar to those in its singlet ground state. (ii) Both exciton bands and band gaps depend on the defect charge. For exciton bands, in the bulk and at the surface, M^- and M^{2-} change the nature of KBr from isolator to semiconductor. (iii) The adsorptivity of atomic H and He was in the range of chemical adsorption. The M-center makes H atom more adsorb. (iv) The HOMO and LUMO levels of the substrate shift to higher energies and band gaps become narrow when M-center is introduced. This change in the electronic structure causes charge transfer between adsorbate and substrate levels.

Key words: KBr, M-center, Excitons, Diffusion, Adsorption, DFT calculations.

Introduction

Charge capture at lattice defects causes optical transitions which absorb light in the transparent perfect crystal. Because many of these absorption bands are in the visible region of the spectrum, they are called color centers [1]. The simplest and most studied color center is the F-center in alkali halides consisting of one electron trapped at a halogen vacancy.

The F_2 (or M)-center consists of two F-centers in the nearest-neighbor positions and it is therefore aligned along $\langle 110 \rangle$ directions in alkali halides and $\langle 100 \rangle$ directions in alkaline earth fluorides and cesium halides. The ground state of the M-center is a singlet state with the electrons on the two vacancies having their spins antiparallel. As a result, it is not possible to observe this states in spin resonance. However, it is possible to create a triplet state with parallel spins of M-center electrons by irradiating at a variety of wavelengths. This triplet states has a long lifetime of a few minutes, then, a sizeable population of triplets can be produced. Electron Paramagnetic Resonance (EPR) and Electron-Nuclear Double Resonance (ENDOR) measurements have been carried out on this metastable triplet and have confirmed the structure of the center [2].

In 1993, Shelimove, et al. [3] carried out *ab initio* calculations of the geometry, electronic structure, ionization and excitation energies of an M-center on the AgBr (001) surface. Jacobsohn, et al. [4] carried out the *Monto Carlo* simulation of the incidence of beams in LiF to provide the dissipated energy and the fluorite ionization depth profiles for comparison with experimental data. F-center formation by monochromatic X-ray has been studied above and below the bromine K-edge in single crystal of KBr at 77 K [5]. In 1999, Losch and Niehus [6] investigated the surface structure of highly insulating KBr (100) by a new technique, impact collision atom scattering spectroscopy with detection of neutrals. So far, there is not enough information about *ab initio* calculations, specially DFT calculations, reported for M-center in KBr. Therefore, we examine bulk and surface properties of M-center diffusion in KBr with particular attention to singlet-triplet crossing and the problem of producing the triplet of M-center.

The indirect way to understanding of the host dependence of band gaps is to start with a model for the host absorption. A complete treatment would involve the theories of excitons [7] and defects [8] which take into account the band structure of alkali halides. This would be a major undertaking and is beyond our present work. Therefore, one has to use the simple electron transfer model of the fundamental optical absorption of ionic solids developed by Hilsch and Pohl [9]. This model, in its simplest form, explains the fundamental

optical absorption as the transfer of an electron from a negative ion to a neighboring positive ion. There is a reasonable agreement between calculations based on Hilsch and Pohl model of exciton and experimental results showed by Bassani and Inchauspe [10]. It seems to be, that all centers have perturbed excitons near them. Theoretically, perturbed excitons near M^{2+} , M^+ , M , M^- and M^{2-} centers have not been studied, although they may give ultraviolet absorption. So, our attention is to examine some of their energetic properties.

Theoretical and experimental studies of adsorbate-substrate interactions have become of increasing importance due to the fact that they are related to variety of technologically significant processes such as catalysis, corrosion, gas sensors, thin-film and semiconductor technology, electrochemistry and molecular electronics. Smooth surface can have point defects, which locally modify the adsorbate-substrate interactions. For studying these interactions computationally and precisely, one has to treat the extended surface when examining a localized phenomenon like chemisorption [11]. Several theoretical studies have been done to simulate adsorption of simple system on ionic surfaces [12]. The M-center is one of several color centers, which was examined by the author for LiH crystal [13-15]. Our theoretical results may serve as predictions because we can not compared to find experimental data due to their absence. A brief summary of the methods and computational details is given in sections 2 and 3. In section 4 the results and discussions are presented.

Crystal Assumption

The treatment of the extended surface when examining a localized phenomenon like chemisorption, is the central process for studying adsorbate-substrate interaction [16]. The optimal way to represent the extended lattice appears to be choosing point ions, which correctly simulate the Madelung potential and its gradient at the active site(s) for chemisorption [17]. To represent the extended crystal properly, some care must be taken for choosing the charges of the point ion. The choice of the appropriate charges for the point ions has been discussed for a FCC structure like MgO [18]. Early studies by Surrat and Kunz [19] and by Clobourn and Mackrodt [20] used clusters, which were terminated by full ionic charges.

To calculate the energies in the crystal under consideration (KBr crystal), we follow a procedure reported for MgO [21] crystal and construct a finite lattice containing 188 point charges. The Coulomb potential along the X and Y-axes of this crystal are zero by symmetry as in the host crystal, Figure 1. The charges on the outer shells (listed in Table 1) are modified to make the Coulomb potential at the four central sites equal to the Madelung potential of the crystal. Also to make the eight points with coordinates $(0, \pm R, \pm R)$ and $(\pm$

$R, 0, \pm R$), where R is half the lattice distance (3.295 \AA for KBr) and equal to zero as it should be in the host crystal. With these charges, 0.409283 a.u. and 0.800909 a.u. , the Coulomb potential in the region occupied by the central ions is very close to that in the unit cell of the host crystal. All charged centers with Cartesian coordinates $\pm X, \pm Y$ and $Z = 2R, 4R, 6R$ and $8R$ are then eliminated to generate a surface of 176 charged centers occupying the three dimensional space $\pm X, \pm Y$ and $-Z = 0, 2R, 4R, 6R$ and $8R$. The coordinates of these charged centers are given in Table 1. Quantum clusters are then embedded within the central region of the crystal surface. All the electrons of the embedded clusters are included in the Hamiltonian of *ab initio* calculations. Other crystal sites are entered into the Hamiltonian as point charges.

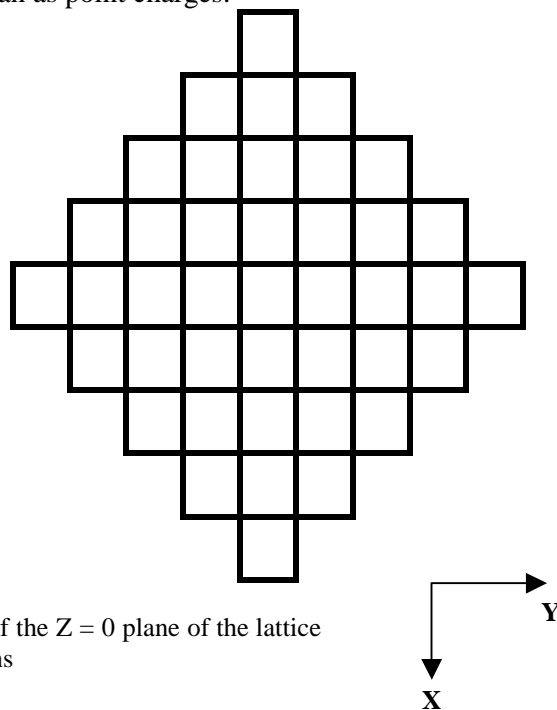


Fig. (1) Representation of the $Z = 0$ plane of the lattice in the calculations

Calculations

To include the M-center in the calculations, one has to consider two electrons trapped in two neighboring anion vacancies along the $\langle 110 \rangle$ axis. For the model under consideration molecular clusters of alkali nuclei at nearest neighbor sites to the two-anion vacancies, with n electrons, consisting of the excess (vacancy-trapped) electrons, plus those associated with the nearest and next nearest neighbor ions. These molecular clusters are then embedded in a lattice of point ions of charge $\pm e$ for alkali or bromide ions.

The adsorption energy ($E_{\text{ads.}}$) of the adsorbate on the surface of substrate is calculated from the relation.

$$E_{\text{ads.}} = E_{\text{complex}} - E_{\text{adsorbate}} - E_{\text{substrate}}$$

The terms appearing on the right hand side are the total energies of the complex (adsorbate + substrate), the adsorbate (free H or He) and the substrate (defect free or defect containing). These terms are obtained from three independent calculations using the same supercell. The negative adsorption energy $E_{\text{ads.}}$ indicates that the bound adsorbate is electronically stable.

Density functional theory (DFT) calculations were performed using Becke's three-parameter hybrid functions with Lee, Yang, and Parr (LYP) correlation functions [22]. This hybrid functional include a mixture of a Hartree-Fock exchange with DFT exchange-correlation. Originally the exchange functional B includes the Slater exchange along with corrections involving the gradient of the density [23] and the correlation functional LYP which includes both local and non-local terms [24]. Stevens, Basch and Krauss introduced Effective Core Potential (ECP) with triple-split basis set Coupled Electron Pair (CEP)-121G [25]. In this work, ECP for K and Br was employed. For bulk cluster such as $\text{Br}_2\text{K}_{14}\text{Br}_3$ with complete interacting electrons, there are 152 basis functions and 324 primitive Gaussians. For surface cluster such as $\text{Br}_2\text{K}_8\text{Br}_2$ with complete interacting electrons, there are 96 basis functions and 208 primitive Gaussians. The calculations are carried out using Gaussian 98 [26].

Results and Discussion

Diffusion of M-center

Due to the presence of point defects, atoms diffuse through crystals at sequence rate providing easy mechanisms for atomic jumps. The M-center diffusion along the $\langle 110 \rangle$ direction is described by five configurations shown as in Fig. (2) The energy required for diffusing M-center in two lattice steps along the $\langle 110 \rangle$ axis may be defined as the energy barriers that must be overcome as the 2F centers jump from one stable site to the next. For 2F centers, there is a little doubt that the relevant saddle point has the migrating Br atom midway between the initial and final position, and the undertaken calculations are based on this assumption. The energetic properties of diffusion for both of the singlet and triplet states in the bulk and at the surface of KBr are presented in Fig. (3) The results confirm that the stability permute between singlet and triplet states for both bulk and surface. On the other hand, the energy barriers for the M-center diffusion were of different values, for instance in the configuration (3); the triplet state is smaller than the singlet state. Therefore, the triplet states of configuration (3) are more stable than its singlet states for both bulk and surface.

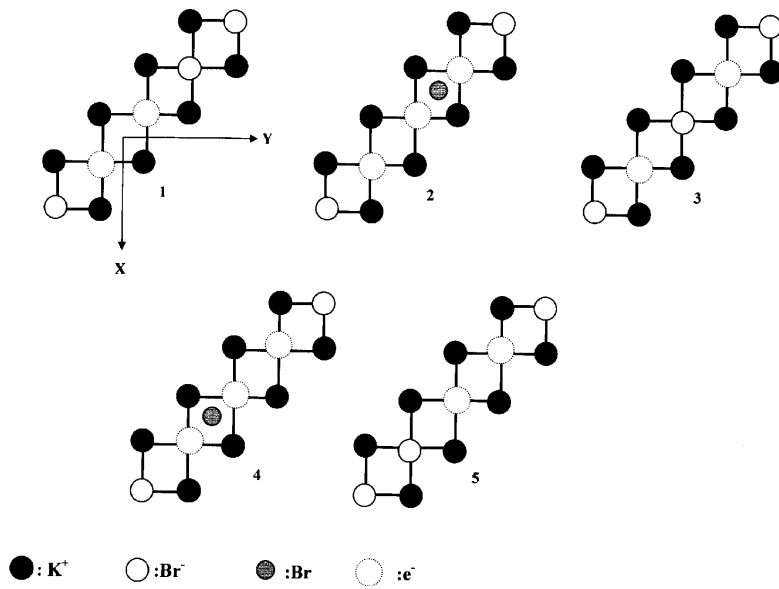


Fig. (2) The diffusion of M-center along $\langle 1-10 \rangle$ direction in KBr. Configuration (1-5).

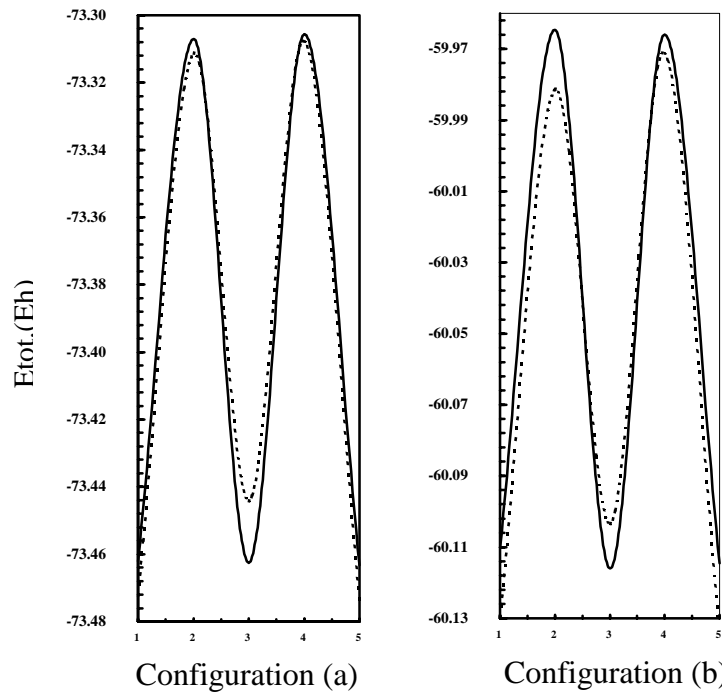


Fig. (3) Energetic properties of M-center diffusion in the bulk (a) and at the surface (b) of KBr crystal.

Band Gaps and Exciton bands

Glasner-Tompkins relation [27] proves the strong dependence of the exciton band and the F-center band on the halide species. Our attention is focused to confirm the relationship between band gaps and exciton bands and the type of the defects [M-center charges (M^{2+} , M^+ , M, M^- and M^{2-})]. The dependence of band gaps and exciton bands on the M-center charges in the bulk and at the surface are given in Table 2. The band gap E_f can be calculated as the difference between valence band (Highest Occupied Molecular Orbital (HOMO)) and the conduction band (Lowest Occupied Molecular Orbital (LOMO)). The exciton band is evaluated as the difference in Coulomb potentials concerning the transfer of an electron from negative ion to a neighboring positive ion (electron-hole recombination); both are placed in the Coulomb field of the simulated crystal. The calculations were carried out for the two central K^+ ions, the defect center surrounded by its nearest neighbor ions as well as the two bromides already placed in the (100) plane, $K_{10}Br_2$ in the bulk and K_8Br_2 at the surface. All ion clusters were surrounded by point charges as defined in Table 1 and the ions were included in the Hamiltonian of *ab initio* calculations. Other crystal sites are entered the Hamiltonian as point charges.

Adsorptivity of Atomic H and He

Indeed, the adsorbate-substrate interactions happen due to the tendency of the adsorbate valence electrons to interact with the available substrate electrons. The influence of this interaction takes place (chemisorption) if there is a small energy gap between adsorbate and substrate electrons, or if the adsorbate has an open shell electronic configuration.

The electrostatic fields near the surface of an ionic crystal are generally large [28]; therefore, the polarization is a major component of the adsorption energy for many physisorbed species. In order to understand the possible electrostatic contribution to the bonding when using K_8Br_4 defect free and K_8Br_2 defect containing surfaces, we calculate the electrostatic potentials on the (0,0,0) site of each cluster. Figure 4, illustrates that, there is a distinction between electrostatic potentials due

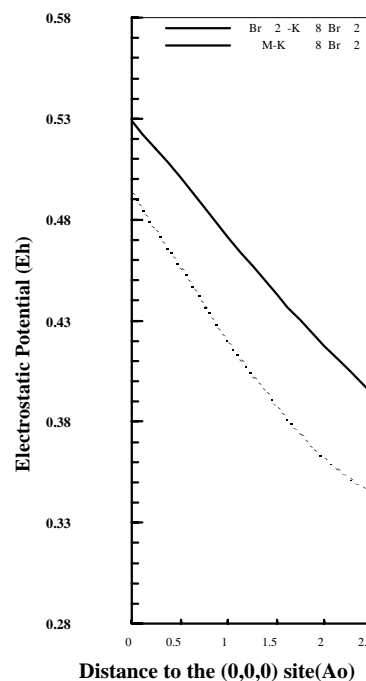


Fig. (4) Electrostatic potentials over the defect free ($Br_2-K_8Br_2$) and defect containing ($M-K_8Br_2$) surfaces of KBr crystal.

to defect free and defect containing M-center (1.01-1.39 eV) at a distances between consider (0.0-2.5 Å), respectively. The shapes of functions are not very similar, this means that one can expect different electric fields and their derivatives. Since the electrostatic interaction of the adatom with the surface will mainly consist of electric field (induced dipole moments) and electric field derivative (induced quadruple moments). One expects that, the classical contributions to the adatom-surface interactions of defect free and defect-containing cluster differ significantly. The introduction of M-center changes the adsorptivity of H atom, while, the adsorptivity of He atom dose not change.

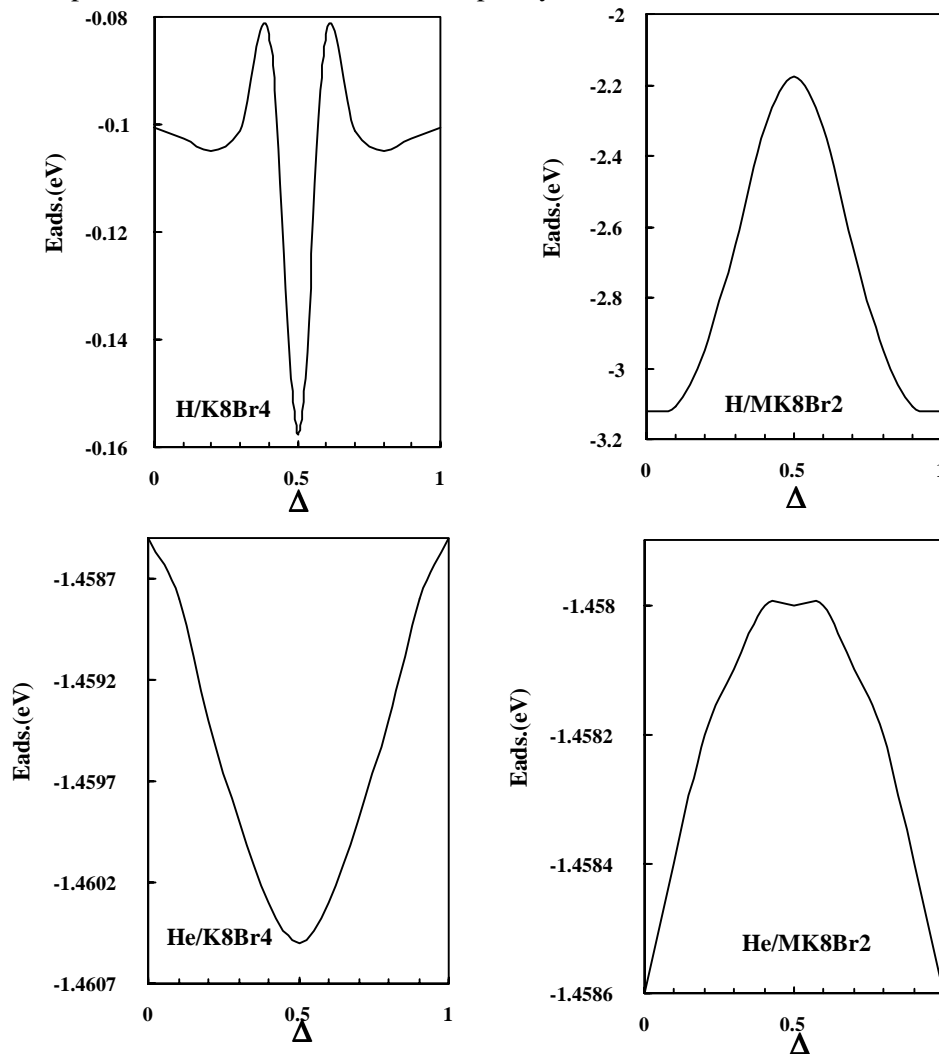


Fig. (5) Adsorption of atomic H and He over KBr surface along the adsorption path Δ .

Fig. (5) represents the results of adsorbate (H and He atoms)-substrate (K_8Br_4 defect free and K_8Br_2 defect containing) interactions. The curves show that, the binding of atomic He at Br^- and F-center are favored than the binding of atomic H at Br^- and F-center for both defect free and defect containing (M-center), respectively. These favored binding occur at the substrate location $\Delta = 0.5$ of the defect free at the substrate location $\Delta = 0.0$ of the M-center defect, Δ being the separation of the 2F-centers (M-center). In the case of M-center defect the binding of atomic He was more favored than the binding of atomic H. Therefore, the M-center restricts significantly the mobility of atomic H over the surface so it does facilitate the mobility of atomic He where less energy barriers exist.

Figure 5 also illustrates the decrease in adsorption energies for adsorbate atomic He when going from the defect free to the defect containing surface. This may be interpreted on the basis of the following: (i) In the defect free surface, the two bromides are localized in their original positions of the lattice surface (despite of the large spatial extension of the electronic charge) and their nuclear charges minimize the repulsion between He and Br^- electrons. (ii) In the defect-containing surface, the non-localized distribution of M-center electrons and the absence of the two bromides nuclear charges maximize the repulsion between He and M-center electrons. Figure 6 shows schematically the unit cells and the path along which the adatom surface distances optimized at selected substrate sites Δ .

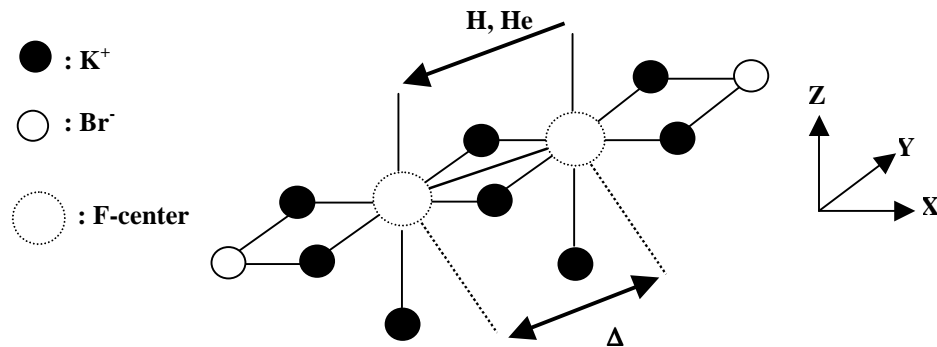


Fig. (6) Characteristics of adsorption energies E_{ads} of atomic H and He over the defect free ($Br_2-K_8Br_2$) and defect containing (M- K_8Br_2) surfaces of KBr crystal along the adsorption path Δ .

To distinguish the differences in adsorption of atomic H and He on the defect free and M-center containing surfaces; one has to calculate the local densities of states (LDOS). The band gaps, which are calculated as the differences between HOMOs and LOMOs of the defect free and M-center

containing surfaces, are given in Table 3. The band gap is reduced by 4.78 eV for the M-center containing surfaces, as a consequence of the HOMO and LOMO shifting to higher energies. The energy levels of hydrogen single occupied and unoccupied atomic orbital were calculated to be -13.56 eV and 2.63 eV, respectively. The energy levels of helium occupied and unoccupied atomic orbital are calculated to be -24.95 eV and 0.56 eV, respectively. Since the charge transfer may occur from, the single occupied atomic orbital of H and the double occupied atomic orbital of He to the substrate unoccupied molecular orbital (donation), or from, the HOMO of the substrate to either the single occupied or unoccupied atomic orbital of H or the unoccupied atomic orbital of He (back donation). These results may support the previous observation that while the adsorptivity of atomic H is drastically increased over the M-center containing surface, the adsorptivity of atomic He was significantly reduced over the same surface.

4.4 Bulk and Surface Relaxation

Because the M-center appears as a charged defect of quantum mechanical nature, it is likely to be associated with local distortions in the lattice. One has to switch on simultaneously inward-outward displacements of the nearest neighbor cations to M-center in addition to the two nearest neighbor bromides in the $\langle 110 \rangle$ plane, in order to shed some light on the optimal relaxation modes. Bulk and surface optimal relaxation modes are found to be associated with simultaneous outward displacements of the surrounding ions as shown schematically in Figure 7. Total energy lowering attributed to simultaneous outward displacements of nearest neighbor ions amount to 0.12% and 0.15% of the total energy in the bulk and at the surface, respectively. The surface relaxation is shown to be more important than bulk relaxation. This is possible attributed to the significant changes in Coulombic interactions between the defect center and its surrounding crystalline potential.

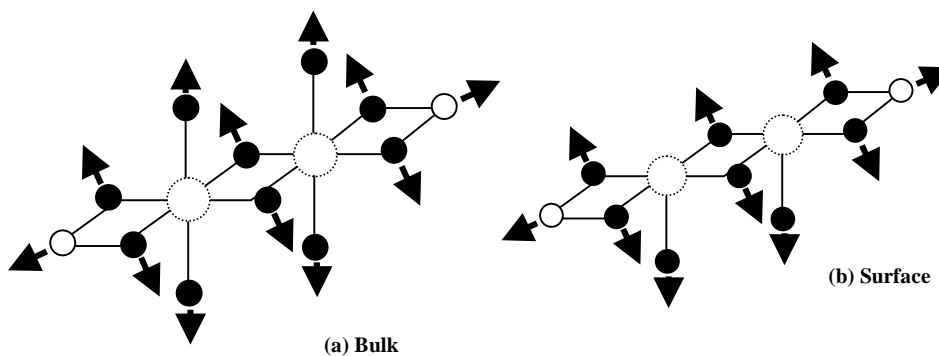


Fig. (7) Relaxation modes of nearest neighbor ions to M-center in the bulk (a) and at the surface (b) of KBr crystal.

Table 1.
Specification of the finite lattice used for crystal bulk and surface calculations. R is half the lattice distance which for KBr is 3.295Å and r is the distance of the appropriate shell from the center of the lattice.

r^2/R^2	Coordinates/R ^(a) X , Y , Z	Number ^(a) of centers	Coordinates/R ^(b) X , Y , -Z	Number ^(b) of centers	Charge q
2	1 1 0	4	1 1 0	4	1
6	1 1 2	8	1 1 2	4	1
10	3 1 0	8	3 1 0	8	1
14	3 1 2	16	3 1 2	8	1
18	1 1 4	8	1 1 4	4	1
18	3 3 0	4	3 3 0	4	1
22	3 3 2	8	3 3 2	4	1
26	5 1 0	8	5 1 0	8	1
26	3 1 4	16	3 1 4	8	1
30	5 1 2	16	5 1 2	8	1
34	3 3 4	8	3 3 4	4	1
34	5 3 0	8	5 3 0	8	1
38	5 3 2	16	5 3 2	8	1
38	1 1 6	8	1 1 6	4	1
42	5 1 4	16	5 1 4	8	1
46	3 1 6	16	3 1 6	8	1
50	5 5 0	4	5 5 0	4	1
50	5 3 4	16	5 3 4	8	1
50	7 1 0	8	7 1 0	8	1
54	5 5 2	8	5 5 2	4	1
54	3 3 6	8	3 3 6	4	1
58	7 3 0	8	7 3 0	8	1
66	5 5 4	8	5 5 4	4	1
54	7 1 2	16	7 1 2	8	0.409283
62	7 3 2	16	7 3 2	8	0.409283
66	1 1 8	8	1 1 8	4	0.800909
82	9 1 0	8	9 1 0	8	0.800909
86	9 1 2	16	9 1 2	8	0.800909

(a): Crystal bulk.

(b): Crystal surface.

Table (2)
Bulk and surface band gaps E_f and exciton bands E_e in KBr. Energies are given in eV.

		E_f	E_e	
Bulk	$\text{Br}_2\text{K}_{10}\text{Br}_2$	6.59	e-	10.79
	$M^{+2}\text{K}_{10}\text{Br}_2$	4.37	$\text{Br}_2\text{K}_{10}\text{Br}_2$	11.61
	$M^+\text{K}_{10}\text{Br}_2$	2.12	e-	11.13
	$M\text{K}_{10}\text{Br}_2$	1.08	$M^{+2}\text{K}_{10}\text{Br}_2$	10.46
	$M\text{K}_{10}\text{Br}_2$	0.40	$e-M^+\text{K}_{10}\text{Br}_2$	9.76
	$M^2\text{K}_{10}\text{Br}_2$	0.32	$e-M\text{K}_{10}\text{Br}_2$	9.71
			$e-M^2\text{K}_{10}\text{Br}_2$	
Surface	$\text{Br}_2\text{K}_8\text{Br}_2$	6.61	$e-\text{Br}_2\text{K}_8\text{Br}_2$	11.04
	$M^{+2}\text{K}_8\text{Br}_2$	3.23	$e-M^{+2}\text{K}_8\text{Br}_2$	11.84
	$M^+\text{K}_8\text{Br}_2$	2.44	$e-M^+\text{K}_8\text{Br}_2$	11.42
	$M\text{K}_8\text{Br}_2$	1.28	$e-M\text{K}_8\text{Br}_2$	10.87
	$M\text{K}_8\text{Br}_2$	0.41	$e-M\text{K}_8\text{Br}_2$	10.44
	$M^2\text{K}_8\text{Br}_2$	0.36	$e-M^2\text{K}_8\text{Br}_2$	10.13

Table (3)
HOMO, LUMO and HOMO-LUMO energies of defected free (Br_2 - K_8Br_2) and defect containing (M- K_8Br_2) surfaces of KBr in eV.

	HOMO	LUMO	HOMO-LUMO
Br_2 - K_8Br_2	-7.4196	-0.5344	-6.0608
M- K_8Br_2	-2.10197	-0.8196	-1.2824

References

1. A. B. Lidiard, in B. Henderson and A. E. Hughes, (eds.), *Defects and their structure in Non-Metallic Solids*, Plenum, New York (1976).
2. H. Seidel, Phys. Lett. **79** (1963) 27.
3. K. B. Shelimove, A. A. Safnov and A. A. Bagatur'yants, Chem. Phys. Lett. **201** (1993) 84.

4. L. G. Jacobsohn, R. A. Nunes and L. C. S. DoCarmo, J Appl. Phys., **81** (1997) 1192.
5. S. M. Ewald, D. L. Brewster and De-Tong Jiang, Nuovo Cimento D, **20** (1998) 853.
6. A. Losch and H. Niehus, Suf. Sci., **420** (1999) 148.
7. R. S. Knox, in: *Theory of excitons*, Academic Press, New York (1963).
8. G. F. Koster and J. C. Slater, Phys. Rev., **95** (1954) 1167; **96** (1954) 1208.
9. R. Hilsch and P. W. Pohl, Z phys. **57** (1929) 145; **59** (1930) 812.
10. F. Bassani and N. Inchauspe, Phys. rev., **105** (1957) 819.
11. F. W. Clinaro and L. W. Hobbs, in: *Physics of Radiation Effects in Crystals*. Ser. Modern Problems in Condensed Matter Science, Ed. R. S. Johnson and A. N. Orlov, North-Holland. Publ. Co. Amsterdam (1986).
12. A. B. Anderson, C. ravimohan and S. P. Mehandru, Surf. Sci., **183** (1987) 438.
13. A. S. Shalabi, Kh. M. Eid, A. M. El Mahdy and M. A. Kamel, J. Phys. and Chem. Solids, **59** (1998) 395.
14. A. S. Shalabi, A. M. El Mahdy, Kh. M. Eid and M. A. Kamel, Model Simul. Matter Eng., **7** (1999) 1.
15. A. S. Shalabi, A. M. El Mahdy, Kh. M. Eid, M. A. Kamel and A. A. El-Barbary, Phys. Rev, **B60** (1999) 9377.
16. E. A. Colbovrn, Reviews of Solid State Sciences, **5** (1991) 91.
17. R. P. Ewald, Z. Physik, **64** (1921) 253.
18. E. A. Colbourn in: *Advances in Solid State Chemistry*, Vol.1, Eds. C.R.A.Catlow, JAI Press, London (1989).
19. G. T. Surrat and A. B. Kunz, Phys. Rev. Lett. **40** (1978) 347.
20. E. A. Colbourn and W. C. Mackrodt, Surf. Sci., **117** (1982) 571.
21. A. S. Shalabi and A. M. El-Mahdy, J. Phys. and Chem. Solids, **60** (1999) 305.
22. A. D. Becke, "Density – Functional Thermochemistry, III. The role of exact Exchange," J. Chem. Phys. **98** (1993) 5648.
23. A. D. Becke, Phys. Rev., **A38** (1988) 3098.
24. B. Miehlich, A. Savin, H. Stoll and H. Preuss, Chem. Phys. Lett. **157** (1989) 200.
25. T. R. Cundari and W. J. Stevens, J. Chem. Phys. **98** (1993) 5555.
26. Gaussian 98, Revision A.6, M. J. Frisch, , et al, Gaussian, Inc., Pittsburgh PA, 1998.
27. A. Glasner and F.C. Tompkins, J. Chem. Phys., **21** (1953) 1817.
28. Z. Guo and L. W. Bruch, J. Chem. Phys., **97** (1992) 7748.